CHARACTERIZATION STUDY OF QUANTUM CRYPTOGRAPHY (QC) BY USING ENTANGLED SOURCE

***Adawiya J. Haider and **Azhar I.Hassen**
Applied Physics Department, University of Technology, Baghdad-Iraq.

*E-mail: adawiya_haider@yahoo.com.
**E-mail: alirose12@yahoo.com.

Abstract

The main goal in Quantum Cryptography is high security and this can be achieved by using single photon sources. The present work is a theoretical analysis devoted to investigate the interference pattern of biphoton amplitude generated by spontaneous parametric down conversion (SPDC) in a nonlinear crystal (BBO) pumped by femtosecond optical pulses. We have studied the visibility as a function of optical path delay for different parameters, such as the crystal length, dispersion in non-linear crystal, pump pulse duration and chirp parameter. The best visibility can be obtained at crystal length of (1.5 mm) .The amplitude of two photons in nonzero dispersion is affected greatly by different crystal length. And the interference pattern is varying with pump pulse duration, the shorter pump pulse duration, the lower visibility (V), and at specific pulse duration the visibility increase with decrease crystal length (L).

Keyword: entangled source; Quantum Cryptography; fs laser ;quantum optics ;quantum information

Introduction

Dispersion plays an important role in the propagation of short classical optical pulses and of quantum wave packets. In particular, transform-limited classical pulses as well as single-photon wave packets Experience temporal broadening upon propagating through a dispersive medium. In classical applications such as communication over optical fibers this pulse broadening ultimately limits the data transfer rates, unless appropriate compensation methods are implemented.

In the case of quantum communications over fibers, the data rates are sufficiently low that such considerations are not necessary. Nonetheless, the presence of dispersive systems in the path between source and detector can compromise certain important quantum phenomena that are central to some of the communications protocols, such as teleportation and dense coding, which rely on entangled photon multiples. [1]

Theoretical Analysis

1. Second Order Dispersion for Entangled Photons:

In this section we are devoted to a theoretical investigation of dispersion effects in fem to second- pulsed SPDC. Particular attention is given to the effects of pump pulse chirp and second orders dispersion (in both the pump and down-converted beams) invisibility and shape of the photo- coincidence pattern. Dispersion cancellation which has been extensively studied in the case cw pumping is also predicted to occur under certain conditions for femtosecond down converted down converted pairs. [2].

We consider a non linear crystal pumped by a strong coherent- state field. Non-linear interaction then leads to the spontaneous parametric down conversion. The two photon amplitude A_{12} depends only on the differences t_1-t and t_2-t. When the down converted beams propagate through a dispersive material of the length l, the entangled two photon state $1\psi^{(2)}>$.

The proposal set up for coincidence- count measurement is shown in Fig. (2) we consider type- II parametric down conversion for this work, using abeam splitter 50/50 and the polarized photons are detected at the detectors D_A and D_B.

In this case two mutually perpendicularly polarized photons are provided at the output plane of the crystal. They propagate through a birefringent material of a variable length *l* and then impinge on a 50/50 beamsplitter. Finally they are detected at the detectors D_A and D_B. The coincidence-count rate R_c is measured by a coincidence device C. The beams might be filtered by the frequency filters F_A and F_B which can be placed in front of the detectors. Analyzers rotated by 45° with respect to the ordinary and extraordinary axes of the nonlinear crystal enable quantum interference between two paths to be observed; either a photon from beam 1 is detected by the detector D_A and a photon from beam 2 by the detector D_B, or vice versa. Including the effects of the beamsplitter and analyzers, the coincidence-count rate R_c can be determined as follows: [3,4]

$$R_c(l) = \frac{1}{4}\int_{-\infty}^{\infty} dt_A \int_{-\infty}^{\infty} dt_B \left|\mathcal{A}_{12,l}(t_A,t_B) - \mathcal{A}_{12,l}(t_B,t_A)\right|^2 \quad \text{.....(1)}$$

The normalized coincidence-count rate R_n is then expressed in the form [2,3]:

$$R_n(l) = 1 - \rho(l) \quad \text{.....(2)}$$

Where

$$\rho(l) = \frac{1}{2R_0}\int_{-\infty}^{\infty} dt_A \int_{-\infty}^{\infty} dt_B \, Re\left[\mathcal{A}_{12,l}(t_A,t_B)\mathcal{A}^*_{12,l}(t_B,t_A)\right] \quad \text{.....(3)}$$

and

$$R_0 = \frac{1}{2}\int_{-\infty}^{\infty} dt_A \int_{-\infty}^{\infty} dt_B \left|\mathcal{A}_{12,l}(t_A,t_B)\right|^2 \quad \text{.....(4)}$$

Let us assume that the nonlinear crystal and the optical material in the path of the down-converted photons are both dispersive.

The wave vectors $k_p(\omega_{k_p})$, $k_1(\omega_{k_1})$, and $k_2(\omega_{k_2})$ of the beams in the nonlinear crystal can be expressed in the following form, when the effects of material dispersion up to the second order are included [5]:

$$k_j\left(\omega_{k_j}\right) = k_j^0 + \frac{1}{v_j}\left(\omega_{k_j} - \omega_j^0\right) + \frac{D_j}{4\pi}\left(\omega_{k_j} - \omega_j^0\right)^2, \; j = p,1,2 \quad \text{.....(5)}$$

The inverse of group velocity $\frac{1}{v_j}$ and the second-order dispersion coefficient D_j are given by [5]

$$\frac{1}{v_j} = \left.\frac{dk_j}{d\omega_{k_j}}\right|_{\omega_{k_j}=\omega_j^0}, \quad \text{.....(6)}$$

$$D_j = 2\pi \left.\frac{d^2k_j}{d\omega_{k_j}^2}\right|_{\omega_{k_j}=\omega_j^0}, \quad j = p,1,2. \quad \text{.....(7)}$$

The symbol ω_j^0 denotes the central frequency of beam j. The wave vector k_j^0 is defined by the relation $k_j^0 = k_j(\omega_j^0)$. Similarly, the wave vectors $\tilde{K}_1(\omega_{k_1})$ and $\tilde{K}_2(\omega_{k_2})$ of the down-converted beams in a dispersive material outside the crystal can be expressed as

$$\tilde{k}_j(\omega_{k_j}) = \tilde{k}_j^0 + \frac{1}{g_j}(\omega_{k_j} - \omega_j^0) + \frac{d_j}{4\pi}(\omega_{k_j} - \omega_j^0)^2, \quad j = 1,2, \quad \text{.....(8)}$$

where

$$\frac{1}{g_j} = \left.\frac{d\tilde{k}_j}{d\omega_{k_j}}\right|_{\omega_{k_j}=\omega_j^0}, \quad \text{.....(9)}$$

$$d_j = 2\pi \left.\frac{d^2\tilde{k}_j}{d\omega_{k_j}^2}\right|_{\omega_{k_j}=\omega_j^0}, \quad j = 1,2, \quad \text{.....(10)}$$

and $\tilde{k}_j^0 = \tilde{k}_j(\omega_j^0)$.

Assuming frequency- and wave-vector phase matching for the central frequencies $(\omega_p^0 = \omega_1^0 + \omega_2^0)$ and central wave vectors $(k_p^0 = k_1^0 + k_2^0)$, respectively. Considering an ultrashort pump pulse with a Gaussian profile: the envelope $\varepsilon_p^{(+)}(0,t)$ of the pump pulse at the output plane of the crystal then assumes the form [6]

$$\mathcal{E}_p^{(+)}(0,t) = \xi_{p0} \exp\left(-\frac{1+ia}{\tau_D^2}t^2\right), \quad \text{.....(11)}$$

where ξ_{p0} is the amplitude, τ_D is the pulse duration, and the parameter a describes the chirp of the pulse [7].

The complex spectrum $\varepsilon_p^{(+)}(z,\Omega_p)$ of the envelope $\varepsilon_p^{(+)}(z,t)$ is defined by

$$\mathcal{E}_p^{(+)}(z,\Omega_p) = \frac{1}{2\pi}\int_{-\infty}^{\infty} dt \mathcal{E}_p^{(+)}(z,t)\exp(i\Omega_p t) \quad \text{.....(12)}$$

For a pulse of the form given in eq. (11) we obtain

$$\mathcal{E}_p^{(+)}(0,\Omega_p)=\xi_p\frac{\tau_D}{2\sqrt{\pi}\sqrt[4]{1+a^2}}\times\exp\left[-\frac{\tau_D^2}{4(1+a^2)}(1-ia)\Omega_p^2\right], \quad ....(13)$$

where $\xi_p=\xi_{p0}\exp\left(\frac{-i\arctan(a)}{2}\right)$.

We arrive at the following expression for the two-photon amplitude

$$A_{12,l}(\tau_1,\tau_2)=\int_{-L}^{0}dz\frac{1}{\sqrt{\beta_1\beta_2-\gamma^2}}\times\exp\left[-\frac{c_1^2\beta_2+c_2^2\beta_1+2\gamma c_1c_2}{4(\beta_1\beta_2-\gamma^2)}\right] \quad ....(14)$$

The functions $\beta_j(z)$, $c_j(z)$, and $\gamma(z)$ are defined as follows [3]:

$$\beta_j(z)=\frac{1}{\sigma_j^2}+b(1-ia)-i\frac{d_j}{4\pi}l-i\frac{D_p-D_j}{4\pi}z,\qquad j=1,2,$$

$$c_j(z)=(-1)^{(j-1)}\left[\left(\frac{1}{v_p}-\frac{1}{v_j}\right)z+\frac{l}{g_j}-\tau_j\right],\qquad j=1,2,$$

$$\gamma(z)=b(1-ia)-i\frac{D_p}{4\pi}z. \quad ....(15)$$

The parameter b is a characteristic parameter of the pump pulse:

$$b=\frac{\tau_D^2}{4(1+a^2)}. \quad ....(16)$$

The quantities $\rho(l)$ and R_0 are then determined in accordance with their definitions in eqs. (2) and (3), respectively. The quantity $\rho(l)$ as a function of the length l of the birefringent material then takes the form ($\omega_1^0=\omega_2^0$ is assumed).

The evaluation of bi-photon amplitude.

$$\rho(l)=\frac{\pi^2|C_A|^2|\xi_p|^2\tau_D^2}{2\sqrt{1+a^2}R_0}\mathrm{Re}\left\{\int_{-L}^{0}dz_1\int_{-L}^{0}dz_2\frac{1}{\sqrt{\overline{\beta_1}\overline{\beta_2}-\overline{\gamma}^2}}\times\exp\left[-\frac{\overline{c_1}^2\overline{\beta_2}+\overline{c_2}^2\overline{\beta_1}+2\overline{\gamma}\overline{c_1}\overline{c_2}}{4(\overline{\beta_1}\overline{\beta_2}-\overline{\gamma}^2)}\right]\right\}. \quad ....(17)$$

The functions $\bar{\beta}_j(z_1,z_2)$, $\bar{c}_j(z_1,z_2)$, and $\bar{\gamma}_j(z_1,z_2)$ are expressed as follows:

$$\overline{\beta}_j(z_1,z_2)=\frac{1}{\sigma_1^2}+\frac{1}{\sigma_2^2}-i\frac{d_j-d_{3-j}}{4\pi}l+2b-i\frac{D_p-D_j}{4\pi}z_1+i\frac{D_p-D_{3-j}}{4\pi}z_2,\qquad j=1,2,$$

$$\overline{c}_j(z_1,z_2)=\left(\frac{1}{v_p}-\frac{1}{v_1}\right)z_j-\left(\frac{1}{v_p}-\frac{1}{v_2}\right)z_{3-j}+\left(\frac{1}{g_1}-\frac{1}{g_2}\right)l,\qquad j=1,2,$$

$$\overline{\gamma}(z_1,z_2)=2b-i\frac{D_p}{4\pi}(z_1-z_2). \quad ....(18)$$

Similarly, the normalization constant $R0$ is given by the expression [8].

$$R_0=\frac{\pi^2|C_A|^2|\xi_p|^2\tau_D^2}{2\sqrt{1+a^2}}\int_{-L}^{0}dz_1\int_{-L}^{0}dz_2\frac{1}{\sqrt{\tilde{\beta}_1\tilde{\beta}_2-\tilde{\gamma}^2}}\times\exp\left[-\frac{\tilde{c}_1^2\tilde{\beta}_2+\tilde{c}_2^2\tilde{\beta}_1+2\tilde{\gamma}\tilde{c}_1\tilde{c}_2}{4(\tilde{\beta}_1\tilde{\beta}_2-\tilde{\gamma}^2)}\right], \quad ....(19)$$

Where

$$\tilde{\beta}_j(z_1,z_2)=\frac{2}{\sigma_j^2}+2b-i\frac{D_p-D_j}{4\pi}(z_1-z_2),\qquad j=1,2,$$

$$\tilde{c}_j(z_1,z_2)=\left(\frac{1}{v_p}-\frac{1}{v_j}\right)(z_j-z_{3-j}),\qquad j=1,2,$$

$$\tilde{\gamma}(z_1,z_2)=2b-i\frac{D_p}{4\pi}(z_1-z_2). \quad ....(20)$$

It is convenient to consider the pump-pulse characteristics at the output plane of the crystal, i.e., to use the parameters τ_D and a. They can be expressed in terms of the parameters τ_{Di} and a_i appropriate for the input plane of the crystal:

$$a=\left(\frac{\tau_{Di}^2a_i}{4(1+a_i^2)}+\frac{D_pL}{4\pi}\right)\left(\frac{\tau_{Di}^2}{4(1+a_i^2)}\right)^{-1},$$

$$\tau_D=\tau_{Di}\sqrt{\frac{1+a^2}{1+a_i^2}}. \quad ....(21)$$

In this case, the parameter b_i

$$b_i = \frac{\tau_{Di}^2}{4(1+a_i^2)} \qquad (22)$$

has the same value as the parameter b defined in eq. (16).

has the same value as the parameter b defined in eq. (28).

Ignoring second-order dispersion in all modes (D_p=D_1=D_2=0), eq. (17) reduces to the following analytical expression for the quantity ρ:

$$\rho(\Delta\tau_l) = \sqrt{\frac{\pi}{2}}\frac{1}{|\Lambda|L}\frac{\tau_{Di}}{\sqrt{1+a_i^2}} \times \mathrm{erf}\left[\frac{\sqrt{2}|\Lambda|}{D}\frac{\sqrt{1+a_i^2}}{\tau_{Di}}\left(\frac{DL}{2}-|\Delta\tau_l|\right)\right], \qquad (23)$$

in which[9]

$$D = \frac{1}{v_1} - \frac{1}{v_2},$$

$$\Lambda = \frac{1}{v_p} - \frac{1}{2}\left(\frac{1}{v_1}+\frac{1}{v_2}\right), \qquad (24)$$

and

$$\Delta\tau_l = \tau_l - DL/2 \qquad (25)$$

The symbol *erf* denotes the error function. When deriving eq. (23), the condition D>0 was assumed. In eq. (25), τ_l denotes the relative time delay of the down-converted beams in a birefringent material of length l and is defined as follows:

$$\tau_l = \left(\frac{1}{g_2} - \frac{1}{g_1}\right) l \qquad (26)$$

In the absence of the second order dispersion and frequency filter a useful analytical expression for two photon amplitude;

$$A_{12,l=0}(t,\tau) = \frac{4\pi\sqrt{\pi}\sqrt[4]{1+a_i^2}}{\tau_{Di}|D|}\mathrm{rect}\left(\frac{\tau}{DL}\right) \times \exp\left[-\frac{1+ia_i}{\tau_{Di}^2}\left(t+\frac{\Lambda}{D}\tau\right)^2\right] \qquad (27)$$

Where t=tA+tA/2,τ=tA-Tb.

The quantity ρ given in eq. (3) then has the form (again it is assumed that $\omega_1^o = \omega_2^o$)

$$\rho(\Delta\tau_l) = \frac{|C_A|^2\sqrt{2\pi}\pi\sigma}{4R_0} \times \mathrm{Re}\left\{\int_{-L/2}^{L/2} dz_1 \int_{-L/2}^{L/2} dz_2\, \gamma_\sigma(z_1,z_2,\Lambda(z_1-z_2)) \times \exp\left[-\frac{\sigma^2}{8}\left(\Delta\tau_l + \frac{D}{2}(z_1+z_2)\right)^2\right]\right\}, \qquad (28)$$

where $\Delta\tau_l$ is defined in eq. (25). The correlation function $\gamma_\sigma(z_1, z_2, x)$ of two pulsed fields at positions z_1 and z_2 is written as

$$\gamma_\sigma(z_1,z_2,x) = \int_{-\infty}^{\infty} dt\, \mathcal{E}_{p\sigma}^{(+)}(z_1 - L/2, t)\mathcal{E}_{p\sigma}^{(-)}(z_2 - L/2, t+x) \qquad (29)$$

The constant R_0 occurring in eq. (28) is expressed as follows:

$$R_0 = \frac{|C_A|^2\sqrt{2\pi}\pi\sigma}{4}\int_{-L/2}^{L/2} dz_1 \times \int_{-L/2}^{L/2} dz_2\, \gamma_\sigma(z_1,z_2,\Lambda(z_1-z_2)) \times \exp\left[-\frac{\sigma^2 D^2}{32}(z_1-z_2)^2\right]. \qquad (30)$$

For a Gaussian pulse with the complex spectrum as given in eq. (13), the correlation function γ_σ becomes

$$\gamma_\sigma(z_1,z_2,\Lambda(z_1-z_2)) = \frac{\sqrt{\pi}\tau_{Di}^2}{2\sqrt{1+a_i^2}}\frac{|\xi_p|^2}{\sqrt{\psi(z_1,z_2)}} \times \exp\left[-\frac{\Lambda^2(z_1-z_2)^2}{4\psi(z_1,z_2)}\right],$$

$$\psi(z_1,z_2) = 2b_i + \frac{2}{\sigma^2} - i\frac{D_p}{4\pi}(z_1-z_2), \qquad (31)$$

Which, together with eqs. (28) and (30), leads to expressions which agree with those derived from eqs. (17) and (19). The parameter b_i is defined in eq. (22).

We have used adaptive Simpson quadrator method to numerically evaluate the double integral in eq.(17) and (28).

Results and Dissociation

In this work, numerical results of the effect of the pump pulse profile (pulse duration and chirp) and the second-order dispersion in both the non-linear crystal and the interferometer's optical elements on the interference pattern are presented.

Most of results developed in this work were extracted from a very sophisticated equation, which has no simple analytical solution. So was been illustrated in previous section, different numerical techniques have used to overcome this problem.

The assumed parameters used in this work are;-single-mode cw argon-ion laser with a wavelength of 351.1 nm, -BaB2O4 (BBO) crystal with a different thickness. The distance between the crystal and the detection planes was 1m.

1- Pump pulse duration and chirp

Studying of quantum interference was with a pump pulse profile (pulse duration and chirp) and second order dispersion in both the nonlinear crystal and interferometer optical elements was presented: We will discuss here a theoretical investigation of dispersion effects in femtosecond- pulsed spontaneous parametric down conversion effects. Particular attention is given to the effects of pump-pulse chirp and second order dispersion (in both the pump and down-converted beams) on the visibility and shape of the photon coincident pattern.

For Fig.(3) Crystal length L=(0.5~10) mm, and ai = 0; values of the other parameters are zero. Values of the inverse group velocities appropriate for the BBO crystal with type-II interaction at the pump wavelength λp=351.1nm and at down-conversion wavelengths $1/v_p=57.05\times10^{-13}$ s/mm, $1/v_1=56.23\times10^{-13}$ s/mm, and $1/v_2=54.2631\times10^{-13}$ s/mm. We assume that the optical materials for the interferometer are quartz, for which $1/g_1$ =51.813 × $^{10-13}$ s/mm and $1/g_2 = 52.08\times10^{-13}$ s/mm.

Fig. (3) shows the relation of an ultrashort pump pulse duration T_{Di} with fringe visibility, it has been shown that ultrashort pumping lead to losses in visibility of the coincidence count interference pattern, and depended on crystal length, while visibility increases with decreased the crystal length and this agreement with the results of references [4, 10]. For example, the highest visibility (0.95) at pulse duration (8×10^{-13}sec) and crystal length (1.5 mm) but visibility is lower at same pump pulse duration but for longer crystal thickness (10mm), as shown in Fig.(3).

2- Second Order Dispersion in the nonlinear crystal

Second-order dispersion in the pump beam causes changes in the pulse phase (chirp) as the pulse propagates and this leads to broadening of the pulse. This pump pulse broadening is transferred to down converted photon. The shape of two photon amplitude shown in Fig.(4). The tilt of the amplitude in the (t, τ) planes leads to a loss in visibility since the overlap of the two amplitudes cannot be completed for non zero tilt. Fig. (4,a,b) shows a peak in the (t- τ) plan for shorter crystal, while this peak disappears at longer crystal.

As illustrated in Fig. (5), the profile of the interference dip is modified as follows: An increase in the second–order dispersion parameter D_p leads to an increase of visibility, but no change in the width of the dip. In Fig.(5) decreasing of pulse duration will reduce the visibility ,for example at $\tau_d=1\times10^{-13}$sec, visibility which measure from coincidence count is smaller than in case of $\tau_d=2\times10^{-13}$sec. and at same value of pulse duration the visibility was higher when second order dispersion D_p is larger than zero as shown in Fig.(5a,b&c) as like R_n =0.55 for D_p=30.

For appropriately chosen values of D_p a small local peak emerges at the bottom of the dip as shown in Fig. (6-a), nonzero initial chirp (a_i) of the pump beam can provide a higher central peak, but on the other hand, it reduces the visibility [as shown in Fig. (6-a & b)]. The peak remains but is suppressed, in the presence of narrow frequency filter. We see from Fig. (6) the dip of interference will be narrower with decreases of crystal length. The dip is very sharp and smoother when L=1.5 mm.

In anther words, the visibility is higher at chirp parameter a_i =0,and reduces with increasing of chirp parameter, while visibility is larger when using small crystal thickness (L=1.5 mm) at the same value of a_i.

In Fig. (6-c), long crystal (L=5 mm) a bearing noise curves of coincident count at chirp parameter ai=1-2, because of high dispersion occure at longer crystal, and this dispersion will reflect on the coincident count behavior.

Conclusion

The dispersion of pump beam before the non-linear crystal does not influence the interference pattern. The interference pattern symmetry increases with decrease pump pulse duration. Second order dispersion of the pump beam in the non-linear crystal can result in occurrence of the local peak at the bottom of the interference dip.

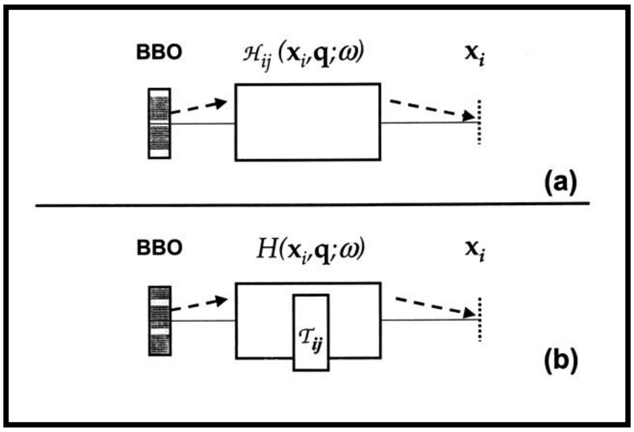

Fig. (1): (a) Illustration of the idealized setup for observation of quantum interference using SPDC [1].

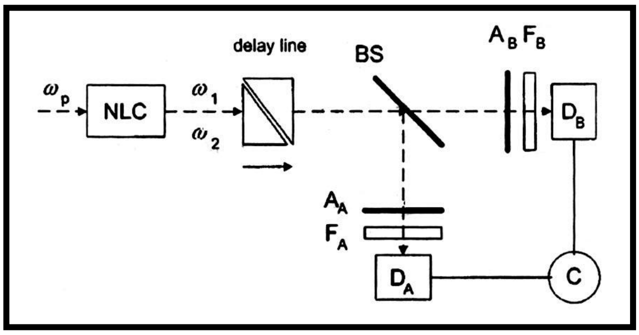

Fig. (2): Sketch of the system under consideration: a pump pulse at the frequency vp generates down-converted photons at frequencies v1 and v2 in the nonlinear Crystal [4].

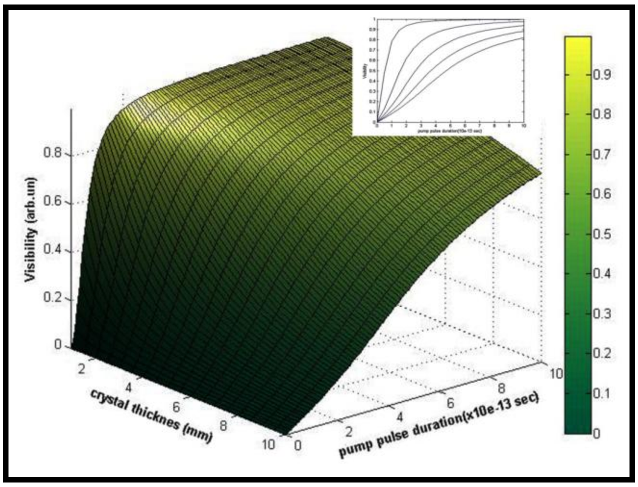

Fig.(3) :Visibility as a function of the pump pulse duration and crystal thickness by using eq.(3.93).

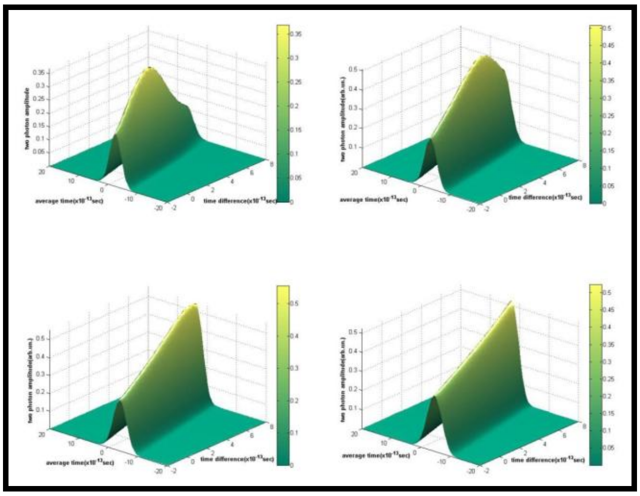

Fig.(4): Absolute value of the two-photon amplitude for nonzero second-order dispersion of the pump beam and for different crystal thickness. L=(a-1.5, b-3mm, c- 5, d-10)mm by using eq.(3.84).

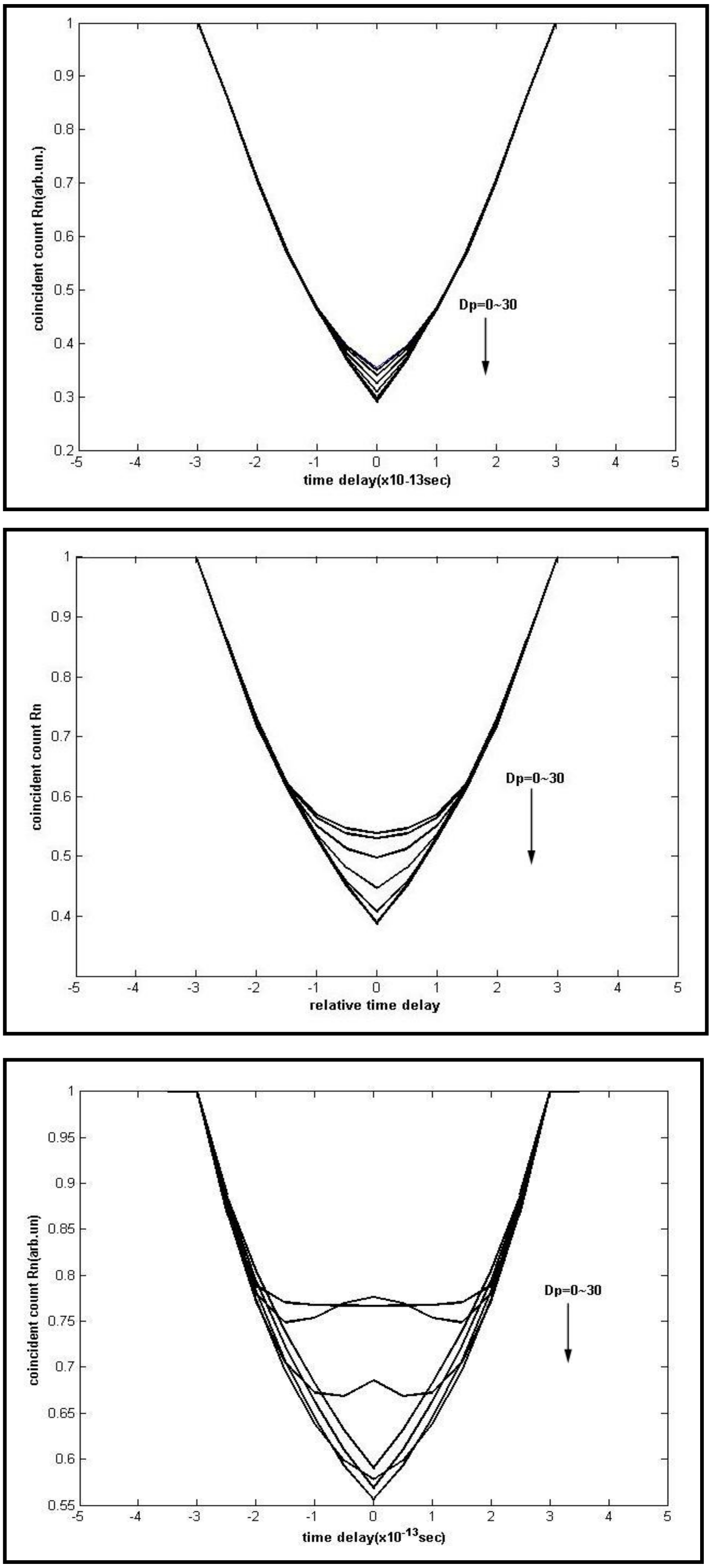

Fig.(5) :Coincidence-count rate $R_n(\Delta\tau_l)$(a) for various values of the second-order dispersion parameter by using eq .(3.72 & 3.98) D_p :D_p=(0, 5×10^{-26} , 1×10^{-25}, 3×10^{-25})s^2/mm . and at pulse duration t_d =(a- 3, b-2, c-1)$\times10^{-13}$sec, ai=0.

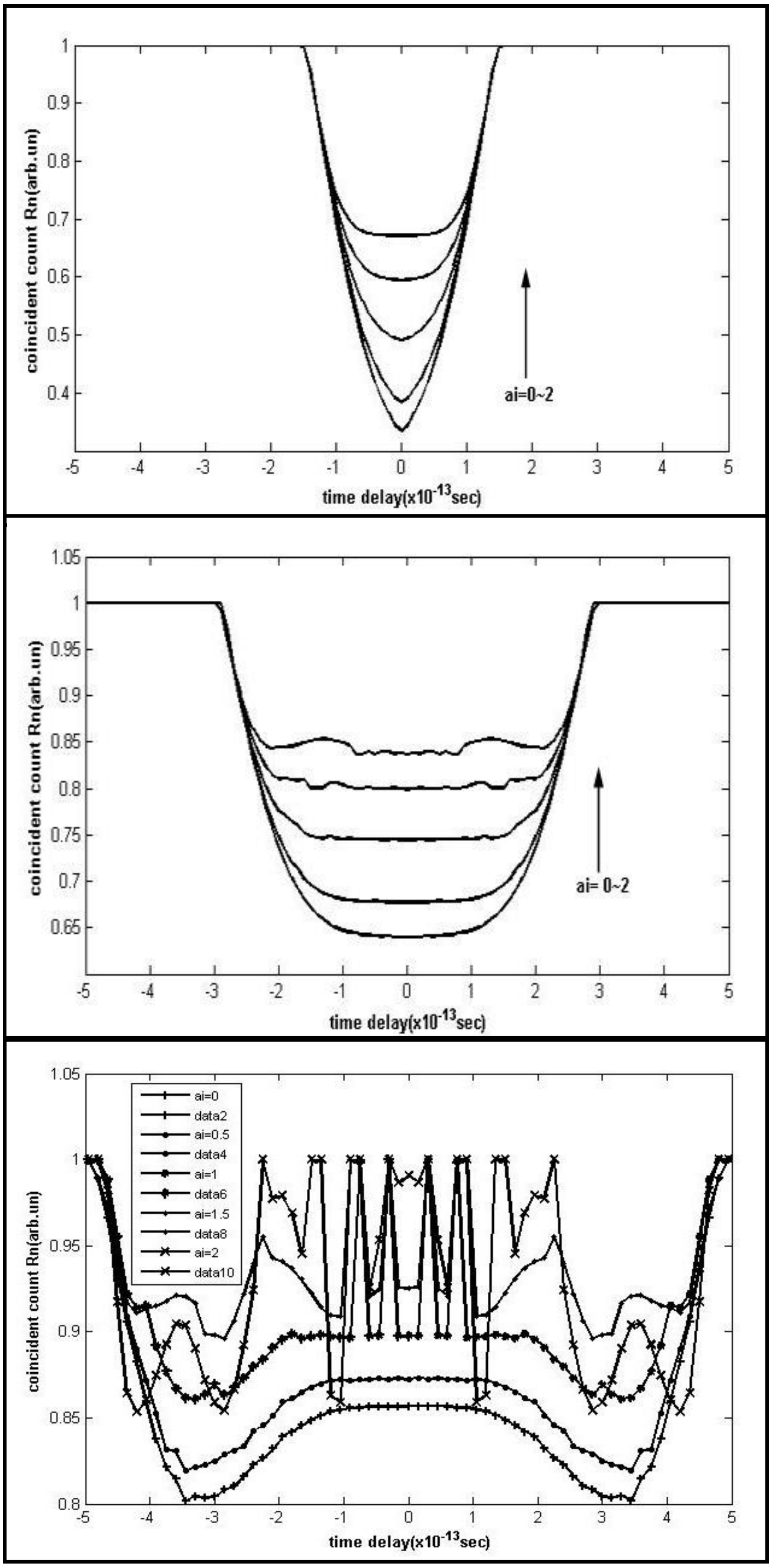

Fig.(6) Coincident count rate as a function of $\Delta\tau_l$ for different chirp value a_i, by using eq .(3.72 & 3.98) ,at L = 1.5 mm, b- L= 3 mm c- L=5mm.

References

[1] Reinhard Erdmann, "Restoring dispersion cancellation for entangled photons produced by ultra short pulses" Physical Review A, Vol. 62, 053810(200).

[2] Yoon-Ho Kim, "Measurement of the spectral properties of the twophoton state generated via type II spontaneous parametric downconversion", OPTICS LETTERS / Vol. 30, No. 8 / April 15, 2005.

[3] Jan perina, Jr., Alexander V. sergienko, Bradley M. Jost,Bahaa E.A. Saleh, and marlin C. Teich, "Dispersion in femtosecond Entangled Two-Photon Interference", Phys.Rev., A, Vol.59, No. 3, (1999).

[4] G. Di Giuseppe, L. Haiberger, and F. De Martini, "Quantum interference and in distinguishability with femtosecond pulses", Phys. Rev. A, Vol.56, No. 1, (1997).

[5] N .Grate & H.Venghaus, "Fiber Optics Communication Device", Springer Verlag, (1998).

[6] Gunther Mahlke & Peter Gossing, "Fiber Optics Cables", Publicis MCD Corporate Publishing, (2001).

[7] Frenc Krausz, Ernst Wintner, "Ultra short light pulse" Lecture notes, Vienna University, 2001.

[8] Ivan Ordavo, "Free-Space Quantum Cryptography", Diploma Thesis, Department für Physik, (2006).

[9] Mete Atatüre, Alexander V. Sergienko, Bahaa E. A. Saleh, and Malvin C. Teich , "Entanglement in Cascaded-Crystal Parametric Down-Conversion ", PHYSICAL REVIEW LETTERS, VOLUME 86, NUMBER 18,(2001).

[10] Claude Cohen – Tannoudji, Bernard Diu, Frank Laloe, "Quantum Mechanics", John Wiely & Sons, (1992).

الخلاصة

تعد السرية العالية هي الهدف الرئيسي في مجال التشفير الكمي التي يمكن الحصول عليها بأعتماد مصادر الفوتونات المفردة ، لدا فقد تمت دراسة مصادر الفوتونات المتشابكة وبيان كيفية تأثير العناصر البصرية لمنظومات التشفير الكمي على معدل حساب التزامن وقابلية الرؤيا . كرست التحليلات النظرية في هده الاطروحة لدراسة نمط التداخل لسعة الفوتونات الثنائية والمولدة بطريقة Spontaneous Parametric Down) SPDC Conversion) في البلورات اللاخطية (BBO) والتي يتم ضخها بأعتماد نبضات ضوئية قصيرة جدا.

درست قابلية الرؤيا كدالة لتأخير المسار البصري ولعدة معلمات مثل طول البلورة ، والتشتت في البلورة اللاخطية. المتشابكة وزمن نبضة الضخ ومعلمة الزقزقة لموجة النبضة ، وقد اظهرت النتائج ان افضل رؤيا يمكن الحصول عليها عندما يكون طول البلورة (1.5 mm) . كما ان سعة الفوتونين في التشتت اللاصفري تتأثر بشكل كبير بطول البلورة ، وأن نمط التداخل يتغير مع زمن نبضة الضخ حيث ان الزمن القصير للضخ يؤدي الى قابلية رؤيا منخفضة ، كما وجد زيادة في قابلية الؤيا مع نقصان طول البلورة عند ازمان نبضة مختلفة.